Journal of Physics and Its Applications

Journal homepage: https://ejournal2.undip.ac.id/index.php/jpa/index



Review Impact of Compressed Breast Thickness and Exposure Parameters on Mean Glandular Dose (MGD) in Full-Field Digital Mammography Examination

Vivi Sumanti Victory¹, Johan Andoyo E. Noor^{1*}, Chomsin S. Widodo¹, Zaenal Arifin²

- ¹Department of Physics, Brawijaya University, Malang, Jawa Timur, Indonesia
- ²Department of Physics, Faculty of Science and Mathematics, Diponegoro University, Jl. Prof. Soedharto, SH., Tembalang, 50275, Semarang, Indonesia

Corresponding author: inoor@ub.ac.id

ARTICLEINFO

Article history: Received: 28 May 2025 Accepted: 1 August 2025

Available online: 27 November 2025

Keywords:
Breast Cancer
Mammography
Compressed Breast Thickness
Mean Glandular Dose

ABSTRACT

The purpose of this paper is to review and summarize the relationship between the average mammary gland dose (MGD) and compressed breast thickness (CBT) in digital mammography. The relationship between MGD and CBT, measured using a dosimeter, shows that the thicker the breast, the higher the MGD. However, the relationship between MGD and CBT using patient data (i.e., actual MGD values) may not be directly proportional to CBT because it can be influenced by other factors, such as age. MGD values are directly proportional to CBT when based on phantom measurements. Across various brands and types of mammography units, MGD values are not always directly proportional due to differences in K patterns (incident air kerma), which create different automatic exposure control (AEC) modes. In conclusion, CBT has a complex relationship with MGD. In general, MGD is positively correlated with CBT because increasing breast thickness requires a higher radiation dose to produce optimal image quality. However, this relationship is not always linear and can be negatively correlated under certain conditions, considering the influence of other parameters that can affect both CBT and MGD.

1. Introduction

Breast cancer is one of the leading causes of death among women globally. Each year, approximately 2.1 million women are newly diagnosed with breast cancer, according to global data [1]. Despite advances in detection and treatment, breast cancer remains the second leading cause of death after cardiovascular disease. Screening using mammography has been shown to reduce breast cancer mortality by up to 25% [2]. However, mammography uses ionizing radiation, which poses a risk to sensitive tissues such as fibroglandular tissue [1,2]. Therefore, accurate radiation dose monitoring is an important aspect of clinical practice.

One of the key indicators in assessing radiation exposure during mammography is the Mean Glandular Dose (MGD), which estimates the average dose absorbed by the breast glandular tissue. MGD is a key indicator in assessing patient safety during imaging procedures. The MGD value can be influenced by various technical parameters such as Compressed Breast Thickness (CBT), breast tissue composition, beam quality (HVL), and exposure settings such as tube voltage (kVp) and tube current-time product (mAs) [3,4].

Among the various factors influencing MGD values, CBT is one of the most significant determinants. As tissue thickness increases, the radiation dose required to maintain optimal diagnostic image quality increases; however, the quantitative correlation between CBT and MGD still shows considerable variability between studies,

depending on the technology, exposure technique, and imaging protocols adopted at each facility [4,5].

Differences in imaging positions also impact CBT values, where the Mediolateral Oblique (MLO) projection usually produces a greater compressed thickness than the Craniocaudal (CC) projection, so the MGD in the MLO projection also tends to be higher [5]. Therefore, modern mammography systems are generally designed to automatically adjust X-ray parameters based on the thickness of the compressed tissue to ensure optimal image quality [6].

This review aims to systematically review the literature on the relationship between CBT and MGD in the context of Full-Field Digital Mammography (FFDM) procedures. Specifically, this review aims to analyze how variations in tissue thickness during compression affect MGD values and to identify other technical parameters contributing to this relationship.

Although numerous studies have highlighted the association between CBT and MGD, significant inconsistencies in the results remain. This variation stems from differences in exposure protocols, mammography system types, and patient anatomical characteristics. Currently, few systematic reviews comprehensively summarize these findings, particularly in the context of FFDM technology. Yet, a thorough understanding of the CBT-MGD relationship is crucial for supporting and optimizing imaging protocols and effective dose control strategies.

The urgency of this review is growing as the adoption of digital mammography technology increases, particularly in developing countries. As the

frequency of routine screenings increases, it is crucial to ensure that radiation doses remain within safe limits without compromising the diagnostic quality of the resulting images.

2. Method

This review was compiled using a narrative approach to synthesize various literature discussing the relationship between CBT and MGD in the context of FFDM examinations. The analyzed studies included patient-based research and laboratory experiments using phantom models. The phantom models used were PMMA, CIRS, 3D Printed Breast Phantom, and PMMA-PE. The digital mammography models used were from GE, Siemens, Hologic, Planmed, and Fujifilm. The dosimeters used were ionization chambers, TLD-100, TLD-200, and BeO. Patient data were obtained from 360 mammography images collected at sample hospitals participating in this study.

The literature search was conducted through four major scientific databases: PubMed, ScienceDirect, Scopus, and Google Scholar. The search process used keywords combined with Boolean operators, including "MGD," "CBT," "Digital Mammography," "Radiation Dose," and "Breast Imaging."

The literature selection focused on publications from between 2010 and 2024, written in Indonesian or English, and accessible in full-text format. Furthermore, the bibliographies of primary articles were also searched for additional relevant sources. Each article was evaluated through a critical analysis of its methodological quality, content relevance, and contribution to understanding the quantitative relationship between CBT and MGD. This analysis also included the identification of other technical factors influencing the relationship.

3. Result and Discussion

The MGD value for various PMMA thicknesses is determined by the equation:

$$D = K \times g \times c \times s \tag{1}$$

Here, *K* is the ESAK on the phantom surface measured without backscatter; *g* is the conversion fa-

ctor that converts air kerma to MGD for a breast with 50% glandularity; *c* is a factor that takes into account glandularities different from 50%; and *s* is a factor introduced due to different anode/filter combinations [7].

Table 1 presents the calculated MGD values using the TLD-100, BeO, and TLD-200 dosimeters and ionization chambers for Mo/Mo target/filter combinations at different PMMA phantom thicknesses. The MGD results obtained from the different dosimeters are correlated. Increasing the PMMA phantom thickness from 2 to 6 cm consistently increases MGD values, as measured using various dosimeter types, including the ionization chamber, TLD-100, BeO, and TLD-200. This finding reflects a linear relationship between phantom thickness and absorbed glandular dose.

For the ionization chamber dosimeter, the MGD was 0.41~mGy at a PMMA phantom thickness of 2 cm, 0.72~mGy at 4 cm, 1.24~mGy at 5 cm, and 2.29~mGy at 6 cm.

The TLD-100 dosimeter showed MGD values of 0.38~mGy at 2 cm, 0.75~mGy at 4 cm, 1.33~mGy at 5 cm, and 2.39~mGy at 6 cm.

The BeO dosimeter showed values of 0.56 mGy at 2 cm, 0.77 mGy at 4 cm, 1.27 mGy at 5 cm, and 2.26 mGy at 6 cm.

Likewise, the TLD-200 showed MGD values of 1.00 mGy at 2 cm, 3.85 mGy at 4 cm, 8.07 mGy at 5 cm, and 17.22 mGy at 6 cm.

The Mean Glandular Dose (MGD) values at various PMMA phantom thicknesses showed an increasing trend with increasing thickness, as detailed in Table 1. Aslar et al.'s study, which used four types of dosimeters (ionization chamber, TLD-100, BeO, and TLD-200), found that the MGD increased from 0.41 mGy at 2 cm PMMA to 17.22 mGy at 6 cm PMMA using TLD-200 [1,9].

This phenomenon indicates a positive relationship between CBT and MGD, which aligns with the basic principles of radiation physics: the thicker the tissue, the higher the radiation dose required to obtain optimal diagnostic image quality.

Table 1: The MGD measurements were obtained using an ionization chamber, TLD-100, BeO, and TLD-200 dosimeters at various PMMA phantom thicknesses.

PMMA Thickness	Ionization Chamber	TLD-100	BeO	TLD-200
(cm)	(mGy) (Aslar, 2020)	(mGy) (Aslar, 2020)	(mGy) (Aslar, 2020)	(mGy) (Aslar, 2022)
2	0.41±0.02	0.38± 0.02	0.56± 0.04	1.00± 0.05
4	0.72±0.04	0.75± 0.02	0.77± 0.04	3.85± 0.18
5	1.24±0.07	1.33± 0.02	1.27± 0.11	8.07± 0.38
6	2.29±0.13	2.39± 0.02	2.26± 0.19	17.22±0.93

However, the variation between dosimeters is significant. For example, the MGD for a 6 cm PMMA phantom ranges from 2.26 mGy (BeO) to 17.22 mGy (TLD-200). This demonstrates the importance of instrument selection in dosimetry research and represents a key limitation when comparing results across studies. Different dosimeters have varying sensitivities and responses to radiation, leading to different reported MGD values. These differences are due to the distinct physical characteristics of each dosimeter type [8].

Ionization chamber detectors offer high accuracy and long-term stability, providing linear and reliable results, but their response is slow compared to solid-state dosimeters [10,11]. The TLD-100 detector is highly sensitive to X-rays, but its energy response depends on tissue composition [12,13]. The BeO detector is an OSL (Optically Stimulated Luminescence) dosimeter that relies on light emission, making it very sensitive to radiation and more resistant to high exposure levels compared to conventional TLDs [1,14]. The TLD-200 detector has very high sensitivity to low radiation doses [7,15].

Therefore, this study highlights the importance of understanding tissue thickness factors, selecting appropriate dosimeter types, and considering their implications for patient safety in mammography radiation dose measurement.

Patient dose evaluation for a new X-ray system or imaging mode can be greatly informed by literature reviews related to CBT. However, a substantial amount of clinical data is required before definitive conclusions can be drawn regarding patient dose. A simple tissue distribution in a breast model can be assumed to be representative of an average population. It is important to note that the average glandular dose in an individual woman's breast can differ significantly (by up to 59%) from the estimate provided by a standard model [10].

Table 2 summarizes five patient-based studies reporting the relationship between CBT and MGD using different mammography systems. Bouwman et al. [8] demonstrated a strong linear correlation between increasing CBT and increasing MGD, with MGD increasing from 1.18 mGy (CBT 20-29 mm) to 4.17 mGy (CBT 80-90 mm). This occurs due to increased scattering and absorption in thicker tissue, which requires a higher radiation dose [12]. In contrast, studies such as those by Dhou et al. and Alahmad et al. demonstrated a more moderate, even nonlinear, increasing trend, reflecting variability in protocol settings, AEC systems, and patient populations [16,29].

Increased scattering and absorption of radiation in thicker tissue can be explained by the exponential law of attenuation, which states that the intensity of an X-ray beam decreases exponentially as it penetrates tissue: $I = I_0 e^{-\mu x}$.

Radiation scattering (especially Compton scattering) becomes more dominant at greater tissue thicknesses. Compton scattering occurs when X-ray photons collide with electrons, producing new photons with different directions and lower energy [10]. The thicker the tissue, the greater the of scattering. Consequently, probability contribution of scattered photons to the total dose increases. Image contrast also decreases due to increased scatter noise. The Automatic Exposure Control (AEC) compensates for this by automatically increasing mAs (milliampere-seconds) or adjusting kVp (kilovolt peak) when detecting thicker CBTs to maintain optimal detector exposure. However, this compensation directly increases the MGD, because a higher mAs results in more photons, and therefore more energy, being absorbed by the glandular tissue [15].

Table 2: Relationship between CBT and MGD values using patient data in the mammography system

No	Study	Mammo	Thickness (mm)	MGD (mGy)
			20-29	1.18
			30-39	1.37
			40-49	1.64
1	Bouwman et al., 2015 [8]	Hologic selenia Dimensions	50-59	2.29
			60-69	3.01
			70-79	3.71
			80-90	4.17
			2.1	0.92
			3.2	1.33
		Fujifilm-Amuletf full field digital mammography	4.5	1.67
2	Sosu et al., 2018 [17]		5.3	1.43
			6	1.48
			7.5	1.88
			9	4.91
			50	1.2
2	rd 11 + 1 2020 [c]	Siemens	51	1.22
3	Khadka et al., 2020 [6]	Mammomat Fusion	59	1.32
			60	1.36
4 Dho		Siemens Mammomat Inspiration	20-30	0.529
	Dhou et al., 2022 [16]		30-50	0.646
		•	50-70	0.898
			< 29 mm	0.711
5	Alahmad et al., 2023 [29]	Hologic selenia Dimensions	30-49 mm	0.793
		<u>-</u>	> 50 mm	1.396

However, a decrease in the average MGD is observed in larger (5-7 cm) fatty breasts, while an increase is seen in smaller (2-3 cm) dense breasts, a phenomenon influenced by age. Age appears to be a confounding factor that can influence MGD, as it is closely associated with changes in glandular composition and breast density. In previous studies, MGD values were consistently lower for subjects aged 64 years and above [6,17]. Similar findings were reported in another study, where patients with a breast thickness of 32 mm in the 40-49 year age group had an MGD value of 1.55 mGy, while a compressed breast thickness of 60 mm in the 50-64 year age group resulted in an MGD of 2.51 mGy [6,18].

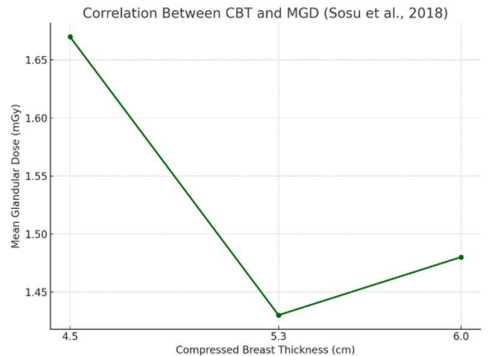


Fig. 1: Graphic Correlation between CBT and MGD (Sosu et al., 2018)

Based on the research results from Sosu et al. (2018), it is explained that the calculated MGD value decreases from a CBT of 4.5 cm to 6.0 cm, which can be seen in Fig. 1. At a CBT of 5.3 cm, the MGD value is 1.43 mGy, which is a decrease from the value at a CBT of 4.5 cm [17]. This reflects a negative or nonlinear correlation within a certain range. The physical cause of this negative correlation can be explained by several factors, namely the influence of AEC (Automatic Exposure Control) compensation, which

regulates kV and mAs parameters. For a certain thickness range, the system may reduce mAs or adjust kVp to avoid overexposure [11,15]. The decreasing g factor in the MGD = K.g.c.s formula when CBT increases, but kerma (K) increases, causing the MGD value to increase or remain the same, depending on the exposure configuration [19].

Table 3 shows that each study used different phantoms, namely CIRS, 3D Printed Breast Phantom, PMMA-PE, and PMMA. Results from these four phantom types indicate that as the CBT value (phantom thickness) increases, the mean glandular dose value produced by the mammography system also increases. Therefore, the thicker the phantom, the more the MGD value tends to increase. This is consistent with the principles of radiation physics, as thicker materials require greater energy for penetration. In conventional mixed-type breast phantoms, an increase in phantom thickness, which indicates a higher ratio of breast glandular tissue, leads to an increase in the breast glandular dose (Mean Glandular Dose), assuming the mass of glandular tissue remains constant [20].

The MGD value measured using a phantom can still represent the MGD value in a patient, but this is limited to breasts with a relatively homogeneous glandular tissue distribution. If the breast is very dense or has large dense areas, as simulated by a large phantom thickness, the AEC system may alter the exposure settings, which correspondingly impacts the MGD. Nevertheless, the use of a phantom provides stable and reproducible MGD measurements.

Phantom thickness and Mean Glandular Dose (MGD) values in mammography examinations are typically calculated based on the assumption of average glandularity of breast tissue. The MGD value is designed to provide an estimate of the radiation dose received by glandular tissue, which is the most radiation-sensitive breast tissue. The use of standard phantoms such as CIRS, PMMA, PMMA-PE, and 3D P-

Table 3: Relationship between MGD Value and PT (Phantom Thickness) using phantom variation

No	Study	Mammo	Phantom	PT	MGD
NO	Study	машно	Phantom	(mm)	(mGy)
Alkhalifah et al.,			40	0.61	
	2018 (5)	Hologic selenia Dimensions	CIRS	50	0.77
	2010 (3)			60	1.12
	Lee et al., 2021	Hologic Selenia Full-Field Digital	3D Printed Breast	40	0.63
2	[30]	Mammography	Phantom	45	0.64
	[30]	Maininography	i nantom	50	0.64
			PMMA-PE	20	0.62
				30	8.0
				40	0.99
3	Bouwman et al.,	Hologic selenia Dimensions		50	1.35
3	2015 [8]			60	1.87
				70	2.38
				80	2.74
				90	3.04
			РММА	21	0.61
				32	8.0
	Douveman et al			45	1.14
Bouwman et al., 4 2015 [8]				53	1.51
			60	1.87	
			70	2.47	
			90	2.62	
5 Asbeutah, et al 2020 (31)	Ashoutah at al	·	·	40	1.23
		GE Senographe Essential	CIRS	50	1.06
				60	0.94

rinted Breast Phantoms helps simulate the characteristics of breast tissue across various thicknesses and glandularity levels [9].

Table 4: Resume Relationship Between Thickness and

Mul	
Thickness (mm)	MGD (mGy)
20	0.44-0.61
40	0.6-0.8
50	0.77-1.35
60	1.1-1.87
70	1.87-2.38
80	2.47
90	3.04

Tables 3 and 4 demonstrate a consistent positive relationship between phantom thickness and MGD values, regardless of the type of phantom used (CIRS, PMMA, PMMA-PE, or 3D printed). Bouwman et al. (2015) noted an increase in MGD from 0.62 mGy (20 mm) to 3.04 mGy (90 mm) [8]. However, the study by Asbeutah et al. (2020) showed a slight anomaly where the MGD decreased from 1.23 mGy (40 mm) to 0.94 mGy (60 mm), possibly due to the influence of the AEC configuration or variations in tissue density within the phantom [28]. Overall, these studies confirm that the effect of CBT on MGD can be effectively simulated using phantoms, but the validity of this simulation is higher for tissues with homogeneous glandularity [20].

Table 5: Relationship between MGD values and Patient

Breast Thickness in mammography variations

Study	Mammo	Thickness	MGD
Study	Maiiiiii	(mm)	(mGy)
		10-19	1
Viana Du at al	GE	20-29	1.8
Xiang Du et al., 2017 [18]		30-39	2.2
2017 [10]		40-49	2
		50-59	1.8
		60	2
		20-29	1.2
Xiang Du et al.,		30-39	1.4
2017 [18]	Hologic	40-49	1.5
2017 [10]		50-59	2
		60	3
		20-29	1
Xiang Du et al.,		30-39	1.2
2017 [18]	Planmed	40-49	1.3
2017 [10]		50-59	2.3
		60	2.5
		20-29	1.8
Xiang Du et al.,	" Siemens	30-39	1.4
2017 [18]		40-49	1.9
		50-59	1.8
		60	1.8

Table 5 compares MGD and CBT for Hologic, GE, Planmed, and Siemens mammography systems. Hologic shows a trend of increasing MGD with CBT (from 1.2 mGy at 20-29 mm to 3.0 mGy at 60 mm), while Siemens shows an inconsistent relationship (remaining constant at 1.8 mGy from 20-60 mm). This difference can be explained by variations in each

system's AEC settings, detector design, and anode/filter combinations [12].

breast dosimetry Many studies on mammography have shown that numerous factors influence MGD. These factors include tube voltage (kV), tube current-time product (mAs), and Half Value Layer (HVL). However, the most significant patientrelated factor is Compressed Breast Thickness (CBT). Several studies have demonstrated that CBT has a substantial effect on MGD in mammography. The Mean Glandular Dose is calculated based on Equation 1, where the relationship between CBT and the incident air kerma (K) is an influential factor, showing a positive correlation with MGD. The mechanism is that a larger CBT, meaning a thicker breast, will lead the mammography equipment's AEC mode to assess a higher density, thus increasing the tube output (mAs). Consequently, this increases the incident air kerma (K) during the mammography procedure. In the Dance model, the g-factor and c-factor relate to CBT in different ways, ultimately affecting the MGD level [22].

In Dance's study, the g-factor was defined as the coefficient that relates incident air kerma (K) to the Mean Glandular Dose (MGD) for a breast with a standard glandular composition of 50%. The breast model in this study was designed using Monte Carlo simulation. The g-factor was calculated as the ratio of the energy absorbed by the glandular tissue to the product of the incident air kerma (K) and the mass of the glandular tissue within the breast model [10, 23].

Under constant K conditions, although a greater breast thickness (higher CBT) can increase the total energy deposited in the glandular tissue, the larger mass of glandular tissue causes the average absorbed dose (in Gy) to decrease. Therefore, the g-factor decreases with increasing breast thickness [10, 23].

In contrast, the c-factor is affected by CBT in the opposite manner. This factor adjusts the MGD based on differences in breast tissue composition, or glandularity. Research shows that thicker breasts typically have lower glandularity. Consequently, a greater CBT leads to an increase in the c-factor due to the reduced glandular density. This adjustment can contribute to an overall increase in the calculated MGD [10, 23]. Furthermore, breast glandularity is affected by age. In older women, glandular tissue tends to be replaced by adipose tissue, which further influences the c-factor and the resulting MGD [12].

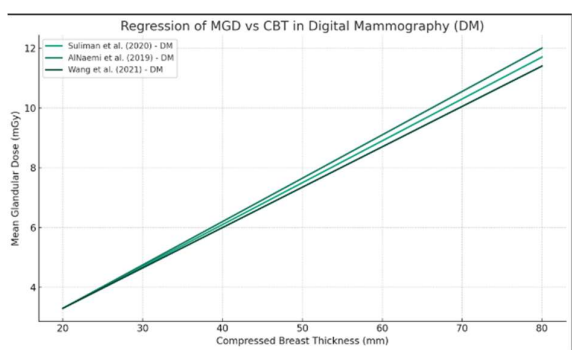


Fig. 2: Graphic Regression of MGD vs CBT in Digital Mammography

Table 6: Regression Model MGD with CBT

Reference	Type	Regression Model
Suliman et al., 2020 (24)	DM	$MGD = 0.13 \times CBT + 0.4$
AlNaemi et al., 2019 (21)	DM	$MGD = 0.135 \times CBT + 0.8$
Wang et al., 2021 (26)	DM	$MGD = 0.13 \times CBT + 0.4$

This linear regression graph, based on the Dance model, shows that MGD is calculated from Equation 1. In this equation, the g-factor, which indicates the ratio of absorbed energy to incident air kerma and glandular tissue mass, tends to decrease with increasing CBT due to the larger tissue volume absorbing the energy more diffusely. Conversely, the *c*-factor increases with decreasing glandularity, which is often associated with increasing age or breast size. The interplay of these two opposing trends causes the relationship between MGD and CBT to be nonlinear [24-27].

Dance et al. and Du et al. reported that despite an increase in CBT, the MGD can decrease for certain tissue types due to reduced glandularity. This phenomenon explains the differences between positive and negative correlations observed across various studies [23,25]. Based on Suliman et al., 2020, it was stated that every 1 mm decrease in CBT reduces the Average Glandular Dose (AGD) by approximately 0.007 mGy in both CC and MLO projections, with a positive correlation value of $r=0.115\ (p=0.049)$ for the Craniocaudal view and $r=0.292\ (p<0.001)$ for the Mediolateral Oblique view [24].

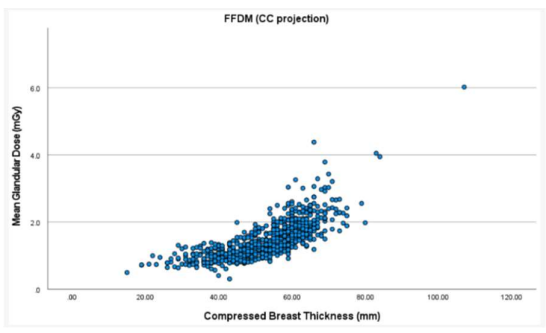


Fig. 3: MGD during FFDM on the CC View (Teoh, et al., 2021) (33)

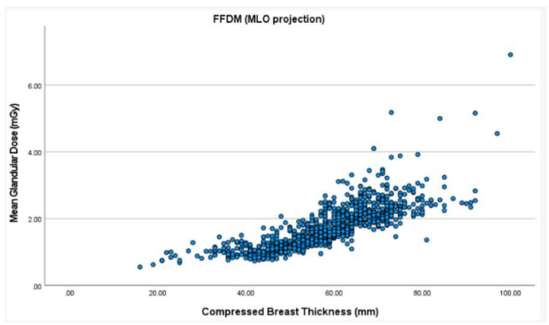


Fig. 4: MGD during FFDM on the MLO View (Teoh, et al., 2021) (33)

Figures 3 and 4 show the results of retrospective and prospective studies that used data from 1208

women, producing 4780 FFDM images in a screening trial to compare MGD [28,33]. MGD is calculated based on the Dance model, where the two main factors affecting radiation dose are breast thickness and breast density [6,32]. Dense breasts consist of a significant amount of glandular and fibrous tissue, while fatty breasts have little glandular tissue and are dominated by adipose tissue. Glandular tissue is more sensitive to radiation than fat tissue; therefore, in breasts with high glandularity, MGD increases more rapidly with increasing CBT [34,35]. This occurs because glandular tissue absorbs more energy, and the AEC system increases the exposure factors (kVp and mAs) to maintain image quality, thereby increasing the total dose. Conversely, fatty breasts with high CBT values and low glandularity can result in a lower MGD [35].

Glandularity changes with age; as age increases, glandular tissue is replaced by fatty tissue, resulting in decreased breast density, commonly referred to as reduced glandularity. Therefore, older women often have low breast glandularity, resulting in low MGD values even at high CBT [36,37].

Figures 3 and 4 illustrate both positive and negative correlations between CBT and MGD. The CC and MLO projections also show that the CC view has a lower radiation dose than the MLO view, likely due to the difference in compressed thickness between the two views [33]. According to Gosch et al., a dose reduction of 20% is achievable when using a selenium detector or a cesium-iodide/amorphous silicon detector [38]. The use of AEC has also been shown to reduce radiation dose compared to manual exposure control. This study demonstrated that image quality using AEC is improved because it minimizes human error in determining appropriate exposure factors for the examination [39,40].

Uhlenbrock (2009) showed that using a tungsten target/rhodium filter (W/Rh) reduced the dose by half compared to molybdenum/rhodium (Mo/Rh). M. Aminah (2010) also found a dose reduction when using W/Rh, followed by Mo/Rh and Rh/Rh. This is due to the higher X-ray spectrum for W/Rh compared to Mo/Rh at the same exposure settings, allowing more photons to reach the detector while breast tissue absorbs fewer photons, thus improving the signal-to-noise ratio and reducing the radiation dose [41,42].

A positive correlation, where thicker CBT requires deeper X-ray penetration—typically depends on high breast gland density (glandularity). However, if mechanical compression is applied optimally, it can reduce CBT, thereby lowering MGD by 25-30% [43,47,49]. According to AlMuhana et al. (2022), CBT is highly positively correlated with MGD (r = 0.68), where the MLO position tends to have a greater CBT and a higher MGD compared to the CC position [44].

A negative correlation between CBT and MGD can occur due to several factors, including the conversion factors in Equation 1, the energy required, target/filter selection (Mo, Rh, W), imaging technique parameters (kVp, mAs, and AEC), breast tissue thickness (where thicknesses greater than 60 mm

generally require a higher MGD), scanning mode (DM/DBT), and technique settings [16,43,47].

In cases of high CBT with high breast tissue density, the risk of under- or over-exposure increases if the AEC is not optimized. Many clinical studies report a positive correlation between MGD and CBT, with r values ranging from 0.5 to 0.7 [46]. In patient-specific 3D modeling, CBT is used as a parameter to construct energy distribution voxels in Monte Carlo simulations. The results show that the dose varies drastically across different CBTs, even with the same kVp, primarily due to the distribution of glandularity [47,50].

Efforts to reduce MGD include applying higher compression forces, which lower CBT, an indirect indicator of breast size.

4. Conclusion

Based on the overall findings, the association between CBT and MGD is generally positive, increasing either exponentially or linearly depending on the technical and biological context. However, complex interactions with factors such as age, tissue density, mammography system, and mathematical models (such as the Dance model) make this association less than universal.

Further studies are needed, particularly in women with dense breast tissue and using tomosynthesis-based mammography systems, to improve the accuracy of personalized MGD estimation. Additional research is also required to assess the effectiveness of various AEC algorithms in reducing MGD without compromising diagnostic accuracy. These research efforts are expected to support the development and validation of more accurate MGD estimation methods, ultimately enhancing patient safety in breast cancer screening.

Acknowledgment

This journal is a literature review, part of a master's degree program conducted by the Department of Physics, Brawijaya University. The author would like to thank the journal for supporting this literature review.

References

- [1] E. Aslar, E. Sahiner, G. S. Polymeris, and N. Meric, "Feasibility of Determining Entrance Surface Dose (ESD) and Mean Glandular Dose (MGD) Using OSL Signal from BeO Dosimeters in Mammography" Radiat. Phys. Chem., 177, 109151, (2020).
- [2] S. Iranmakani, T. Mortezazadeh, F. Sajadian, M. F. Ghaziani, A. Ghafari, et al., "A Review of Various Modalities in Breast Imaging: Technical Aspects and Clinical Outcomes" Egypt. J. Radiol. Nucl. Med., 51, 57, (2020).
- [3] M. E. Suleiman, P. C. Brennan, and M. F. McEntee, "Mean Glandular Dose in Digital Mammography: A Dose Calculation Method Comparison" J. Med. Imaging, 4(1), 013502, (2017).
- [4] I. I. Suliman, S. Mohamed, A. Mahadi, and E. Bashier, "Average Glandular Dose (AGD) and Radiation Dose Optimization in Screen-Film and

- Digital X-Ray Mammography" Appl. Sci., 13(21), 11901, (2023).
- [5] K. Alkhalifah and A. Brindhaban, "Investigation of Exposure Factors for Various Breast Composition and Thicknesses in Digital Screening Mammography Related to Breast Dose" Med. Princ. Pract., 27, 211–216, (2018).
- [6] A. Khadka, A. Jha, R. K. Chaudary, and S. L. Shrestha, "Relationship of the Mean Glandular Dose with Compressed Breast Thickness in Digital Mammography" Nepal. J. Radiol., 10(15), 11–15, (2020).
- [7] D. R. Dance, C. L. Skinner, K. C. Young, J. R. Beckett, and C. J. Kotre, "Additional Factors for the Estimation of Mean Glandular Breast Dose Using the UK Mammography Dosimetry Protocol" Phys. Med. Biol., 45, 3225–3240, (2000).
- [8] R. W. Bouwman, R. E. van Engen, K. C. Young, G. J. den Heeten, et al., "Average Glandular Dose in Digital Mammography and Digital Breast Tomosynthesis: Comparison of Phantom and Patient Data" Phys. Med. Biol., 60, 7893–7907, (2015).
- [9] E. Aslar, "Characterization of CaF2:Dy (TLD-200) Dosimeters and Determination of Dosimetric Quantities in Mammography" Radiat. Meas., 154, 106779, (2022).
- [10] J. A. Seibert and J. M. Boone, "X-Ray Imaging Physics for Nuclear Medicine Technologists. Part 2: X-Ray Interactions and Image Formation" J. Nucl. Med. Technol., 33(1), 3–18, (2005).
- [11] J. T. Bushberg, J. A. Seibert, E. M. Leidholdt, and J. M. Boone, The Essential Physics of Medical Imaging 3rd ed. Lippincott Williams & Wilkins, (2011).
- [12] F. H. Attix, Introduction to Radiological Physics and Radiation Dosimetry Wiley-VCH, (2004).
- [13] Y. S. Horowitz, Thermoluminescence and Thermoluminescent Dosimetry CRC Press, (1984).
- [14] G. S. Polymeris, G. Kitis, and C. Furetta, "Advances in Optically Stimulated Luminescence of BeO and its Applications in Radiation Dosimetry" Radiat. Meas., 46(12), 1346–1353, (2011).
- [15] S. W. S. McKeever, M. Moscovitch, and P. D. Townsend, Thermoluminescence Dosimetry Materials: Properties and Uses Nuclear Technology Publishing, (1995).
- [16] S. Dhou, E. Dalah, R. AlGhafeer, A. Hamidu, and Abdulmunhem, "Regression Analysis Between the Different Breast Dose Quantities Reported in Digital Mammography and Patient Age, Breast Thickness, and Acquisition Parameters" J. Imaging, 8, 211, (2022).
- [17] E. K. Sosu, M. Boadu, and S. Y. Mensah, "Determination of Dose Delivery Accuracy and Image Quality in Full-Field Digital Mammography" J. Radiat. Res. Appl. Sci., 11, 232–236, (2018).
- [18] X. Du, N. Yu, Y. Zhang, and J. Wang, "The Relationship of the Mean Glandular Dose with Compressed Breast Thickness in

- Mammography" J. Public Health Emerg., 1, 32, (2017).
- [19] R. E. Hendrick, "Radiation Doses and Cancer Risks from Breast Imaging Studies" Radiology, 290(2), 284–292, (2019).
- [20] D. L. Miglioretti, J. Lange, J. J. van den Broek, C. I. Lee, N. T. van Ravesteyn, D. Ritley, et al., "Radiation Induced Breast Cancer Incidence and Mortality from Digital Mammography Screening: A Modelling Study" Ann. Intern. Med., 164, 205– 214, (2016).
- [21] H. M. Al-Naemi, O. B. Taha, A. O. Al-attar, M. A. Tarabieh, I. I. Abdallah, N. A. Iqelian, and A. E. Aly, "Evaluation of Mean Glandular Dose from Digital Mammography Exams at Qatar and Compared with International Guidelines Levels" Br. J. Med. Med. Res., 14, 1–9, (2016).
- [22] C. Pwamang, E. Sosu, C. Schandorf, M. Boadu, and V. Hewlett, "Assessment of Dose to Glandular Tissue of Patients Undergoing Mammography Examination" J. Radiol. Radiat. Ther., 4, 1062, (2016).
- [23] D. R. Dance, K. C. Young, and R. E. V. Engen, "Estimation of Mean Glandular Dose for Breast Tomosynthesis: Factors for Use with the UK, European and IAEA Breast Dosimetry Protocols" Phys. Med. Biol., 59, 427–437, (2014).
- [24] N. I. N. Suliman, R. Supar, and H. Sharip, "Effect of Compressed Breast Thickness on Average Glandular Dose (AGD) During Screening Mammography Using Full Field Digital Mammography (FFDM)" J. Acad. UiTM, 8(1), 34– 44, (2020).
- [25] H. M. Al Naemi, A. Aly, A. J. Omar, A. Al Obadli, O. Ciraj Bjelac, M. H. Kharita, and M. M. Rehani, "Evaluation of Radiation Dose for Patients Undergoing Mammography in Qatar" Radiat. Prot. Dosim., 189(3), 354–361, (2020).
- [26] L. Wang, X. Zhou, J. Liu, Y. Li, and Y. Zhang, "Quantitative Imaging Techniques and Dose Estimation in Mammography" J. X-Ray Sci. Technol., 29(1), 85–95, (2021).
- [27] J. E. Baek, B. J. Kang, S. H. Kim, and H. S. Lee, "Radiation Dose Affected by Mammographic Composition and Breast Size: First Application of a Radiation Dose Management System for Full-Field Digital Mammography in Korean Women" World J. Surg. Oncol., 15, 38, (2017).
- [28] S. P. Zuckerman, E. F. Conant, B. M. Keller, A. D. A. Maidment, B. Barufaldi, S. P. Weinstein, M. Synnestvedt, and E. S. McDonald, "Implementation of Synthesised Two-Dimensional Mammography in a Population-Based Digital Breast Tomosynthesis Screening Program" Radiology, 281, 730–736, (2016).
- [29] H. Alahmad, K. AlEnazi, A. Alshahrani, G. R. Alreshaid, S. Albariqi, and M. Alnafea, "Evaluation of Mean Glandular Dose from Mammography Screening: A Single-Center Study" J. Radiat. Res. Appl. Sci., 16, 100749, (2023).
- [30] D. Y. Lee, Y. I. Jo, and S. H. Yang, "Development of Breast Phantoms Using a 3D Printer and Glandular Dose Evaluation" J. Appl. Clin. Med. Phys., 22(10), 270–277, (2021).

- [31] A. M. Asbeutah, A. Brindhaban, A. A. AlMajran, and S. A. Asbeutah, "The Effect of Different Exposure Parameters on Radiation Dose in Digital Mammography and Digital Breast Tomosynthesis: A Phantom Study" Radiography, 26, e129–e133, (2020).
- [32] C. R. Jeukens, U. C. Lalji, E. Meijer, et al., "Radiation Exposure of Contrast-Enhanced Spectral Mammography Compared with Full-Field Digital Mammography" Invest. Radiol., 49, 659–665, (2014).
- [33] K. C. Teoh, H. A. Manan, N. M. Norsudiin, and I. H. Rizuana, "Comparison of Mean Glandular Dose Between Full Field Digital Mammography and Digital Breast Tomosynthesis" Healthcare, 9(12), 1758, (2021).
- [34] Z. A. S. Hegian, L. M. Abu Tahoun, R. M. Ramli, and N. Z. Noor Azman, "Relationship Between Mean Glandular Dose and Compressed Breast Thickness by Age Groups (40–49, 50–64, 65–80)" Radiat. Prot. Dosim., 200(1), 25–31, (2024).
- [35] S. Kunosic, D. Ceke, M. Kopric, and L. Lincender, "Determination of Mean Glandular Dose for Two Age Groups" HealthMED, (2010).
- [36] M. N. M. Norazman, R. M. Ramli, and S. Z. S. S. Aziz, "Patient-Specific Mean Glandular Dose Estimation in Digital Mammography Using the Volpara Method" Diagnostics, 14(22), 2568, (2024).
- [37] A. El Sayed, R. E. El Shiekh, S. M. Yousef, and M. I. Kora, "Evaluation of Patient Dose and Risk in Digital Mammography for Patients in Sudan" Alexandria J. Med., 59(1), 42–48, (2023).
- [38] P. C. Gotzche and M. Neilson, "Screening for Breast Cancer with Mammography" Cochrane Database Syst. Rev., 4, CD001877, (2001).
- [39] S. Uchiyama, H. Suzuki, H. Ueda, and K. Ueda, "Comparison of Different Exposure Modes in Full-Field Digital Mammography: Phantom Study for Automatic Exposure Control Versus Manual" Jpn. J. Health Phys., 46(2), 148–155, (2011).
- [40] G. Tartarotti et al., "Image Quality and Dose Stability of AEC Mode in Mammography and Breast Tomosynthesis Across Different Manufacturers: A Phantom-Based Comparative Study" Eur. Radiol. Exp., 8(1), 16, (2024).
- [41] D. F. Uhlenbrock and T. Mertelmeier, "Comparison of Anode/Filter Combinations in Digital Mammography with Respect to the Average Glandular Dose" Georg Thieme Verlag KG Stuttgart. New York, 181(3), 249–254, (2009).
- [42] M. Aminah, K. H. Ng, B. J. J. Abdullah, and N. Jamal, "Optimal Beam Quality Selection Based on Contrast to Noise Ratio and Mean Glandular Dose in Digital Mammography" Australas. Phys. Eng. Sci. Med., 33, 329–334, (2010).
- [43] Y. Hristova-Popova, A. M. Teneva, M. P. Yordanov, and N. D. Mitev, "Investigation of Glandular Dose in Mammography: Influence of the Breast Glandularity and Compression Thickness" Radiat. Phys. Chem., 181, 109305, (2021).

- [44] A. AlMuhanna, S. M. Yousef, H. S. AlRammah, and S. M. AlDosari, "Evaluation of Patient Radiation Dose During Mammographic Examination" Radiography, 28(1), e102–e109, (2022).
- [45] C. Dance, S. Christofides, A. Maidment, I. McLean, and K. Ng, "Dosimetry in Diagnostic Radiology: An International Code of Practice" IAEA Hum. Health Ser., 23, Vienna: IAEA, (2011).
- [46] N. Moshina, G. G. Waade, M. Roman, S. Sebuodegard, and S. Hofvind, "Subjective Versus Fully Automated Mammographic Density Assessment in the Norwegian Breast Cancer Screening Program" Eur. Soc. Radiol., ECR, C-0618, (2017).
- [47] M. M. Alakhras, C. Mello-Thoms, R. Bourne, M. Rickard, J. Diffey, and P. C. Brennan, "Radiation Dose Differences Between Digital Mammography and Digital Breast Tomosynthesis are Dependent on Breast Thickness" in Proc. SPIE Med. Imaging, 9783, San Diego, CA, USA, (2016).
- [48] A. Merad, S. Saadi, and N. Khelassi-Toutaoui, "Comparison of Two Full Field Digital Mammography Systems: Image Quality and Radiation Dose" in AIP Conf. Proc., 1994, 060008, New York, NY, USA: AIP Publishing, (2018).
- [49] N. Jamal, K. H. Ng, and D. McLean, "A Study of Mean Glandular Dose During Diagnostic Mammography in Malaysia and Some of the Factors Affecting It" Br. J. Radiol., 76, 238–245, (2003).
- [50] P. J. Allisy-Roberts and J. Williams, Farr's Physics for Medical Imaging 2nd ed. Elsevier Health Sciences, (2020).